AN ABSTRACT OF THE THESIS OF

Levi J. Suryan for the degree of Master of Science in Mechanical Engineering presented on November 3, 2016.

Title: A Performance Comparison of Chainsaw Bar Lubricants

Abstract approved:

_____

John P. Parmigiani

Chainsaws, an indispensable tool for modern forestry operations, rely on bar lubricant to prevent rapid wear of the chain and bar. Choice of bar lubricant must balance performance, cost, and biological impact. Many bar lubricants are available, but little published work exists that conclusively ranks the performance of these choices. This study used a series of laboratory-based cutting and free running chainsaw experiments to compare the lubrication performance of 6 petroleum based lubricants and 2 vegetable based lubricants. The cutting experiments mimicked normal operating conditions and used bar temperature distribution to show how lubricant choice, lubricant flowrate and chain tension effected frictional power dissipation in the chain and bar assembly. Cutting results indicated that chain tension was the strongest predictor of frictional power dissipation. Boundary lubrication conditions occurred at 1 mL/min of lubricant flowrate, mixed lubrication occurred at 3-5 mL/min flowrate, and film lubrication occurred at 10 mL/min flowrate. In the 3-5 mL/min flowrate range, high viscosity index appeared to reduce lubricant film breakthrough. The free running experiments used measurements of chain length

increase to test the ability of each lubricant to protect chain components from rapid wear under abusive operating conditions sometimes encountered in the field. Length increase is caused by material loss at the rivets of the chain. Results showed that under these operating conditions, lubricant viscous properties had no effect on wear rates. Lubricant additive composition dictated chain wear rates, which was independent of whether the lubricant was petroleum or vegetable based. The combined results show that a reliable means of evaluating chainsaw bar lubricants was developed and that both high and low quality examples of petroleum and vegetable base lubricants exist.

Presented November 3, 2016

A Performance Comparison of Chainsaw Bar Lubricants

by
Levi J. Suryan

A THESIS

submitted to

Oregon State University

in partial fulfillment of
the requirements for the
degree of

Master of Science

November 3, 2016
Commencement June 2017

Master of Science thesis of Levi J. Suryan presented on November 3, 2016

APPROVED:

Major Professor, representing Mechanical Engineering

Head of the School of Mechanical, Industrial, and Manufacturing Engineering

Dean of the Graduate School

I understand that my thesis will become part of the permanent collection of Oregon State University libraries. My signature below authorizes release of my thesis to any reader upon request.

Levi J. Suryan, Author

ACKNOWLEDGEMENTS

I would like to start by thanking Dr. John Parmigiani for advising me through my graduate studies. He taught me numerous lessons spanning the range of technical, professional, and personal. He pushed me to be efficient while providing enough space for me to learn.

Additionally I would like to thank my committee members Dr. John Nairn and Dr. Rajiv Malhotra for providing high quality instruction, as well as their help in wrapping up my studies. Another thank you goes to my GCR, Dr. Camille Palmer. Another thank you is due to Matthew Cunnington, who helped keep this project moving with his interest, diligence and patience.

My sincere gratitude also goes to Dr. Nancy Squires. Her ability to counsel and inspire me has been utterly instrumental throughout my studies at OSU, and has put me on a path I would not have been able to find without her.

I also extend my thanks to Bernie Viray, whose help in the laboratory as well as his incredible friendship have been so valuable. We kid around a lot, but this is sincere. Another thank you goes to Andrew Otto, whose excellent work laid the foundation for what I was able to do here. I feel fortunate that this project was a good excuse to become his friend.

I would also like to express my boundless appreciation to Jenna Schardt. Her encouragement and input are thoughtful and valuable, and her companionship has kept me on my feet.

My education has not taught me the words for expressing the depth of my gratitude to my family. My parents Cindy and Mark, as well as my sister Sara, have given me unwavering support paired with sage advice that has allowed me to become a capable person.

TABLE OF CONTENTS

Page

LIST OF FIGURES

Figure Page

LIST OF FIGURES (Continued)

Figure Page

LIST OF TABLES

Table Page

Chapter 1: Introduction

Due to their portability and performance, chainsaws are an indispensable tool in forestry operations. While chain mounted cutters were first seen in the medical field in the form of the osteotome as early as 1830 [1], the first patent for a commercial woodcutting chainsaw appeared in 1918 [2]. In the western United States and Canada, the forestry industry began experimenting with chainsaws in the 1930's and recognized their superiority to manual felling by the end of the 1940's [3][4]. From this point forward into the 1980's, the main motivations in chainsaw development were to increase cutting performance and maneuverability. This was achieved with improvements to internal combustion engine technology, and an array of work dedicated specifically to the cutting process of chain-mounted cutters.

Modern chainsaw development has increased motivation for efficiency, durability, and minimized environmental impact. Higher efficiency of the cutting system (consisting of the guide bar, chain, and drive sprocket) allows for smaller, cheaper and more maneuverable power sources, as well as lower fuel consumption. Increased durability of the cutting system also reduces costs in forestry operations. Environmental benevolence in forestry operations is a growing concern. Bar and chain lubricant receive particular attention in this area because they are a 'total loss lubricant,' meaning by design, all of the lubricant consumed is dispersed into the surrounding environment [5]. It has been shown that 64% of the dispersed lubricant is entrained in sawdust, with the remainder adhering to the cut surfaces, falling to the

ground, or becoming aerosolized [6]. Austria directly banned the use of petroleum based chainsaw bar lubricants in 1991 [7]. Germany, France and the UK have placed more general restrictions on forestry lubricants that affect chainsaw bar lubricant choice, while Scandinavian countries have employed tax exemptions to spur biolubricant usage [7]. Meanwhile chain and bar lubricant has been shown to account for 16% of total operating costs in thinning operations using handheld saws [8]. Also of concern are energy efficiency, machine component life, and lubricant service life. These are important factors in both the ecological and economic impact of a chosen lubricant [9]. Biodegradable lubricants appear to have similar performance to petroleum based counterparts, but are generally have higher unit cost. The conflict between lubricant cost and biological impact is strong enough to cause problems; in Germany a 2 million liter annual deficit between approved lubricant purchases and forestry lubricants consumed indicates widespread use of illegal alternatives that are cheaper and higher toxicity [10][11]. These concerns raise the importance of bar lubricant selection, particularly so for professional forestry workers.

Determining a proper lubricant for an application falls within the field of tribology, the study of interacting surfaces and wear. Prerequisite to describing lubricant performance is understanding the types of motion involved in the chain and bar assembly. There are three general categories of surface interaction that will be evaluated in this work: sliding between the guide bar and chain surfaces, sliding between chain surfaces, and rolling within the roller bearing installed in the nose of most guide bars.

The sliding interface between the guide bar and chain is shown in Figure 1. This chain cuts a 0.25” wide kerf, which is typical of handheld chainsaws. Drive links of the chain fit into a groove on the perimeter of the bar, with the groove being composed of two rails. The bar exhibits a roughly elliptical profile, allowing some normal force to be maintained along the chain’s paths between the nose sprocket and drive sprocket. In the absence of any lateral vibration of the chain and bar assembly, the most noteworthy sliding contact occurs between the bottom surfaces of links on the chain, referred to here as chain link heels, and the top of the guide bar rails. The link heels are shown in Figure 2.

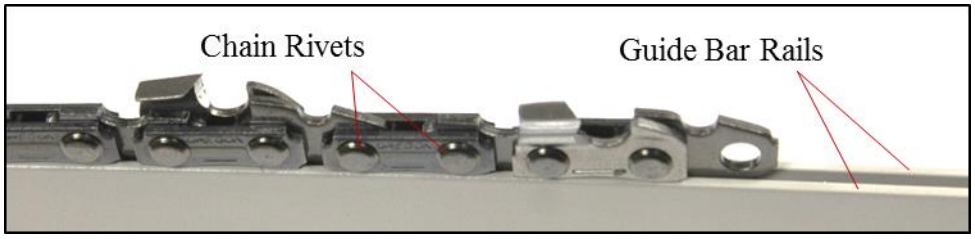

Figure 1: Sliding interfaces of the chain and guide bar. Guide bar rails are visible on the right side of the photo.

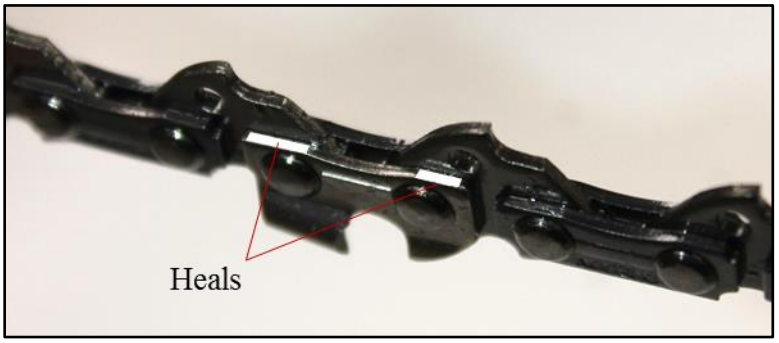

Figure 2: View of the underside of a chain showing chain link heels marked in white. These are the chain’s main bearing surface for sliding interface with the guide bar.

The planar motion assumption is defensible under free running conditions, but harder to verify while cutting is occurring. Using these assumptions the pressure distribution of a lubricant film between each chain link heel and its respective bar rail can be expressed by the Reynolds equation reduced with a narrow bearing approximation, as shown in Eq. 1 [12]. The Reynolds equation is a restriction of the Navier-Stokes equation that is specialized for lubricant films.

$$p = \frac{3\,U\eta}{h^3}\frac{dh}{dx}\left(y^2 - \frac{L^2}{4}\right) \tag{1}$$

Here p is the local pressure in the film (assumed constant through the thickness), U is the sliding velocity of the chain link in the x direction (see Eq. 2), η is the lubricant dynamic viscosity, h is the local film height, y is the lateral distance from the contact centerline, and L is the film width. The integral of pressure distribution over film area defines the total normal load carried by the bearing. It can be seen that if a decrease in the sliding velocity, lubricant viscosity, or the wedge effect of the bearing geometry occurs, the film can compensate with a reduction in thickness up to the point that bearing surfaces begin directly contacting.

The relative velocity U of the chain to guide bar sliding contact is given by Eq. 2 in ft/s. Here n is the number of teeth on the drive sprocket, S is the driveshaft speed in customary units of rev/min, and P is the pitch of the chain in inches. Saw chain pitch is defined as the mean distance between rivet centers, since most chains have alternating short and long chain links. Further, drive sprocket teeth interface with every drive link, so two chain pitches pass for every sprocket tooth.

$$U = \frac{nPS}{360} \tag{2}$$

Normal force exerted at the contact between the link heel and guide bar rail contacts is nominally low along the rail length; this is because tension carried by the chain requires high curvature in the chain's path to be converted to normal force on the guide bar rails. However, feed force can marginally increase this value where the chain and bar system meets the workpiece. Furthermore, the transition experienced by the chain links from high angular velocity on the nose and drive sprockets to low angular velocity in the bar groove occurs over a very short distance of chain travel. The necessary angular acceleration on the links is exerted mainly by normal force on the guide bar, creating rapid wear regions during chainsaw usage (see Figure 10). The areas of highest curvature in the chain's path are on the nose and drive sprockets, which are both supported by roller bearings and therefore are not considered in the chain-to-guide bar surface interaction case.

The category of sliding between chain surfaces can also be greatly reduced by ignoring transverse displacements out of the plane of the guide bar. This is not defensible in the region where the chain passes through the workpiece, due to the asymmetry of the alternating left-hand and right-hand cutters of a modern hooded cutter chain. However it becomes more feasible during free running and also during cutting when considering the locations of the chain's path that are removed from the workpiece. Assuming motion stays in the plane of the bar, the main surfaces of interest are the shaft formed by each rivet in the chain, and the journal which is the

bore through the drive link that captures that rivet. Figure 3 shows a chain link used to join the chain into loops along with a free end of chain. The large diameter centered along the length of the rivet acts as the journal, and the exposed hole in the un-joined drive link forms the bearing.

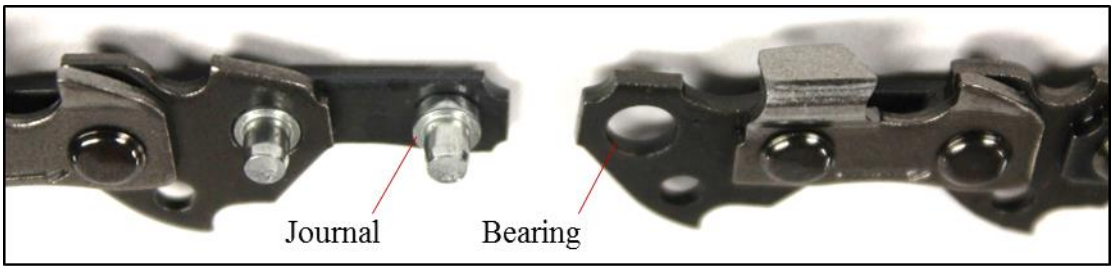

Figure 3: Exposed bearing surfaces at a chain rivet.

The hydrodynamic film pressure in this bearing can be described by a polar version of the Reynolds equation reduced by the narrow bearing approximation, as shown in Eq. 3 [12].

$$p = \frac{3\,U\eta\varepsilon\,\sin\theta}{Rc^2(1+\varepsilon\,\cos\theta)^3}\left(y^2 - \frac{L^2}{4}\right) \tag{3}$$

Here c is the bearing clearance, measured as the difference between journal and bearing radii, and ε is the eccentricity ratio, measured as the distance between journal and bearing centers over the bearing clearance c. However this equation only applies for a developed lubricant film in a continuously rotating journal bearing. Rotation at a rivet is caused by relative angular displacement of two serial links. Thus the angular displacement history of a rivet depends on the chain velocity U, chain pitch P, and the local rate of change of curvature in the chain's path. Approximating

the path of the chain as two straight sections connecting arcs having the effective radii of the nose and drive sprockets yields a useful simplification. Eq. 4 gives the calculation for effective sprocket radius, r_s. Assuming each chain link transitions from zero angular velocity to sharing the angular velocity of the sprocket in one pitch length shows that only in four discrete locations along the chain's path do rivets experience any appreciable rotation: entering and leaving the drive sprocket, as well as entering and leaving the nose sprocket. This means the rotation is oscillatory, intermittent, and only sweeps a small angle. A 6 tooth drive sprocket results in approximately $\pi/6$ radians of total rotation at each rivet. This type of motion will not easily develop a hydrodynamic lubricant film for the chain components.

$$r_s = nP \tag{4}$$

Tension carried by the chain determines the loading of these journal bearings. Chain tension varies with position in the chain since shaft power provided at the drive sprocket is dissipated along the chain's path. Chain tension is highest in the region where it enters the drive sprocket, and lowest while leaving the drive sprocket. This power dissipation view accounts for time-averaged load carried by the chain, but does not account for instantaneous forces caused by oscillation. The time averaged maximum chain tension, where the chain enters the sprocket, can be estimated as the sum of static chain tension and drive shaft torque divided by the effective drive sprocket radius r_s. Furthermore, the equivalent driveshaft torque due solely to cutting of the workpiece can be estimated by multiplying r_s with the force exerted by the

chain on the workpiece in the direction of chain motion at the cut (F_{cut}). The proportion of this equivalent torque to total driveshaft torque T while cutting can be represented by R_{cut} in percent, is shown in Eq. 5. This ratio is equivalent to the ratio of power consumed by cutting to total shaft power consumed by the moving chain.

$$R_{cut} = \frac{100\ F_{cut}\ r_s}{T} \tag{5}$$

The nose bearing of the guide bar also dissipates power. This bearing has an abnormally thin aspect ratio in order to fit within the width of the kerf cut by the chain. Power dissipation occurs at the nose due to rolling contacts that carry radial load in the bearing, as well as sliding contacts that correct misalignment in the bearing thrust direction (which is normal to the plane of the guide bar).

Measurements pertaining to the film are difficult to make while running a chainsaw. An alternative to these measurements is to monitor power dissipation along the chain's path using temperature. Temperature measurements on macroscale components do not suffer from the high frequency (100-5000 Hz) mechanical noise that is inherent to the chainsawing process, giving them an advantage over force measurements. However, history dependence of the temperature distribution does create additional constraints on the test procedure. Power dissipation Q within any bearing causes conversion of shaft power to heat and can be expressed as the product of the sliding velocity U, bearing normal force N, and equivalent friction coefficient k as shown in Eq. 6.

$$Q = UNk \tag{6}$$

Meanwhile, friction coefficient varies widely depending on what type of lubrication regime is occurring, as described by the Stribeck curve. An adaptation of the Stribeck curve is shown in Figure 4 with lubrication regimes denoted by I, II, and III. The boundary lubrication regime (I) is characterized by high friction coefficients and corresponding high wear rates, because microscopic asperities on bearing surfaces are continuously in contact. Friction and where rates under boundary lubrication are dictated by additives in the lubricant, with this variability denoted by the shaded region in Figure 4. Film lubrication (III) relies on viscosity of the lubricant to completely isolate bearing surfaces from physical contact. Component wear rates are expected to be low in this regime, but large amounts of viscous drag can create an elevated friction coefficient. The mixed lubrication regime (II) accounts for intermittent asperity contact in the transition between boundary and film lubrication.

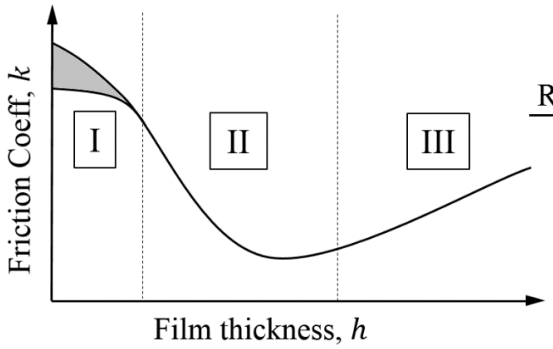

Regime	Frictional Loss	Wear Rate
I	High	High
II	Med to Low	Med
III	Med	Low

Figure 4: Stribeck curve adapted from [7]. Regime I is boundary lubrication, where solid contact controls friction and wear. Regime III is film lubrication, where lubricant creates viscous drag and isolates solid surfaces from contact. Regime II is mixed lubrication, the transition between the two.

Film thickness can also be decreased by lubricant starvation. The pressure developed in hydrodynamic bearings creates a nonzero leak rate which requires sufficient lubricant supply to sustain a film. The method of lubricant supply for the chain and guide bar assembly is quite indirect and is prone to causing starvation. Lubricant is pumped into the groove of the guide bar where the bar is mounted to the drive motor. Lubricant flowrates of 5 to 15 mL/min are typical for handheld chainsaws. This lubricant is then entrained by drive links of the chain and allowed to distribute throughout the chain's path.

Chapter 2: Literature Review

Numerous studies have been published on the biological, chemical and tribological properties of potential guide bar lubricants. Anand and Chhibber [13] delineate between toxicity and biodegradability as determinants of lubricant biological impact. They note that while both toxicity and biodegradability are more favorable for lubricants using vegetable versus petroleum base stocks, the choice of lubricant additives is also critical. Additionally, vegetable base oils are renewably sourced, further decreasing their biological impact [5].

Chemical compatibility also presents an important set of constraints on lubricant choice. Hydrolytic and oxidative stability are a lubricant's ability to resist chemical breakdown on exposure to water and oxygen, respectively. These properties become important due to elevated temperatures and potential contamination in lubricant films employed by the forestry machinery. Vegetable bases tend to underperform compared to petroleum bases in terms of hydrolytic stability [7], but can be improved upon with proper additive choice as shown by Li et al [14]. Salimon et al [15] remark that oxidative breakdown of vegetable bases tends to be rapid and can result in increased acidity and viscosity in the lubricant. They improved upon the thermal oxidative stability as well as the viscosity index of their vegetable base stock via chemical modification. Rac and Vencl [5] also improved upon the oxidative stability of a sunflower based oil developed specifically for chainsaw bar lubrication using an antioxidant additive. While these metrics of chemical stability are important

in the general comparison of lubricants, it was pointed out by Bart [7] that their pertinence to total loss lubrication systems such as chainsaws is limited due to low residence time.

Tribological properties of interest include viscosity and its temperature dependence, along with performance under boundary lubrication conditions which is dictated chiefly by lubricant additives. Vegetable bases exhibit higher viscosity index than petroleum bases, allowing tighter control of viscosity throughout the operating temperature range of the application [13]. Rac and Vencl [5] compared the wear resistance of their sunflower based lubricant with a commercial petroleum counterpart using a block-on-ring tribometer. Measurements of friction coefficient indicated boundary lubrication under the prescribed test conditions. Friction coefficient and lubricant temperatures were lower for the sunflower lubricant than the petroleum lubricant, and conversely material loss on the wear surfaces was lower for the petroleum lubricant. They concluded that the overall wear-prevention ability of both lubricants were comparable.

Separate from studies specifically on the properties of potential bar lubricants are those that evaluate chainsaw performance. As previously mentioned, numerous studies have been aimed at improving the cutting performance of chainsaws. Randel [4] introduced one of the first chainsaw performance studies using a test stand in a laboratory setting in order to compare cutter designs. Wood properties, cross section shapes, chain speeds and feed forces were controlled. Electrical power consumption

of the drive motor was successfully used to compare the chainsaw cutter designs under study. Oehrli [16] also developed a method of comparing and developing chainsaw cutters. Machinability of the workpieces was first tested using a standard circular saw in order to successfully normalize for variation in cutting forces caused by heterogeneous wood properties. The test apparatus could accommodate chainsaw cutters both mounted to a chain and mounted to a rigid disk, showing the decrease in performance of chain-mounted cutters due to lack of rigid constraint and friction between the chain and guide bar. Pahlitzsch [17] added to the understanding by constructing a test stand that measured reaction forces exerted by the chain on the workpiece. Priest [18] measured the performance of entire handheld chainsaws including their internal combustion engines by controlling chain speed and feed force, then recording fuel consumption per area of wood cut. Gambrell and Byars [19] were able to record the cutting force history of a single chainsaw cutter as it passed through the work by rigidly mounting it to a rotating beam. Reynolds et al [20] were able to use measurements of drive torque and reaction forces on the workpiece to predict engine power requirements as a function of drive shaft speed. Naylor et al [21] showed that cutting forces in wood machining can be accurately predicted using mechanical toughness and strength properties for the specific wood specimen being cut. Otto and Parmigiani [22] used an automated chainsaw test stand to determine optimum depth of cut and motor torque requirements for small handheld saws. The typical variables being measured by these cutting studies, namely the drive torque, feed force, and cutting force, have been useful in improving the cutting process.

However these variables struggle to indicate power dissipation due to friction internal to the chain and bar assembly, and the component wear that accompanies it.

Collecting information about power dissipation and friction along the path of the chain is made difficult by the remoteness of a moving chain link. Stacke [23] broke into this problem using a dynamical simulation of the forces and motion of chain links during cutting, and substantiated those results with a set of physical tests. However these models were developed using a Coulombic friction model, which did not allow them to account for variables critical to lubrication performance and wear prevention.

Previous researchers concerned with power dissipation due to friction in the chain and guide bar have resorted to thermal measurements at selected locations on the guide bar. This allows elevated temperatures to indicate higher friction coefficients in the chain and bar assembly, given proper variable control. Stanovský et al [24] measured the effect of lubricant choice on temperature at selected locations on the bar during operation of conventional handheld chainsaws. Temperature measurements were taken using a Fluke Ti25 thermal imager, which can detect temperatures on surfaces of known emissivity to ±3.6 °F with a 160 by 120 pixel detector. The lubricants under study were Stihl BioPlus vegetable based guide bar lubricant and previously used Shell Helix Ultra VX 5W-30 engine lubricant. Measurements were taken after timed intervals of both free running and continuous bucking cuts conducted by a forestry technician. The study was not able to discern a

difference in thermal profiles for the two lubricants, and concluded that the lubricant performances were roughly equivalent. While this study did well at mimicking actual usage of a handheld chainsaw, the inconclusive results may have been due to insufficient variable control. The point locations taken from thermal images in order to reduce the temperature field data from 2-dimensional to 0-dimensional (simplifying statistical comparisons) seem to have been hand selected, which can cause error due to the operating temperature gradients on a guide bar. Thermal images of the entire chainsaw resulted in pixel density of approximately 3.3 pixels per inch, which could also artificially smooth the true guide bar temperature profile. Finally, lack of an automated cutting sequence most likely added unaccounted for variance in frictional heating between test runs.

Nordfjell et al [25] conducted a restricted version of the previous study in a laboratory setting, using a chainsaw test stand capable of free running only. The test apparatus was able to control parameters that are critical to lubricant performance: chain speed, the reaction force between the drive sprocket and guide bar (which controls “static” chain tension), and lubricant flow rate. It used a rubber wheel rolling on a chain having all cutters removed in an effort to mimic cutting conditions. Two vegetable based lubricants and one petroleum based lubricant were compared. Temperature measurements were taken using a single, fixed sensor placed near the guide bar rail interfacing with the low tension (top) strand of chain after set time intervals. This method was able to discern temperature differences between the

lubricants under test. Temperatures were highest for the vegetable based lubricant having the highest viscosity index (242), and lowest with the second vegetable lubricant. The petroleum based lubricant produced temperatures between these extremes.

A study conducted by De Caro [26] collected data on a group of handheld chainsaws used in forestry operations in France in order to evaluate the performance of vegetable versus petroleum based lubricants in a more general context. As expected from the previous two studies listed, performance differences between lubricant types were difficult to discern due to lack of variable control. It was noted that under cutting conditions that were tough for the chain and bar, some of the vegetable based lubricants could not control guide bar temperatures and hindered chainsaw operation. Using SEM micrographs and roughness measurements, they also concluded that vegetable based lubricants out performed petroleum counterparts because chain link bearing surfaces were smoother. This conclusion may have missed the mark; highly polished bearing surfaces can also indicate higher occurrence of boundary lubrication and rapid component wear, depending on the original state of the bearing surfaces.

Chapter 3: Cutting Test Apparatus, Methods and Consumables

This chapter describes the apparatus, methods and consumables used for the lubricant comparison tests that incorporated cutting. This testing aimed to measure changes in the guide bar temperature distribution due to bucking cuts under a variety of conditions for each lubricant. The test apparatus for performing the cuts is the same as described in detail by Otto [22], with some particular modifications (described below) to facilitate the current research goals. The mechanical subsystems are labeled in Figure 5. Not shown are the machine enclosure or automation and data acquisition systems. Data acquisition for all force and torque measurements was carried out at 2.0 kHz during cutting and free running of the chain.

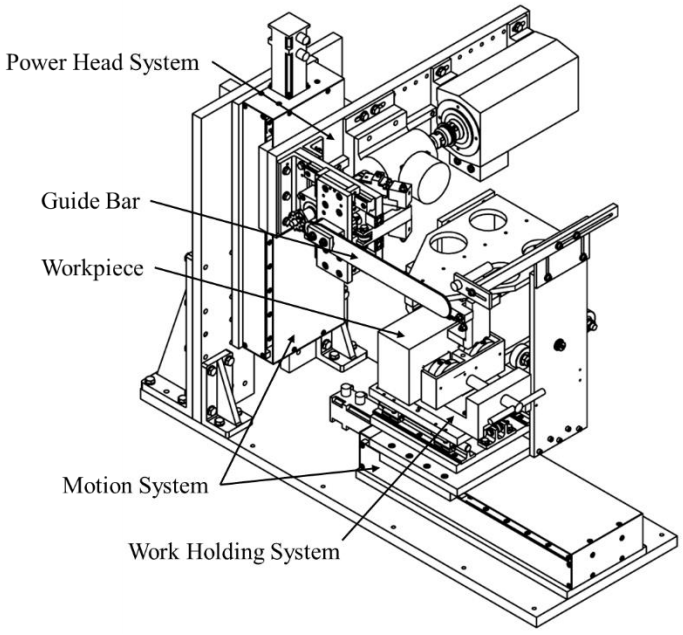

Figure 5: Mechanical subsystems of the chainsaw test stand.

The motion system consists of two linear axes used for feeding the chain through the workpiece. Only the vertical axis was employed for bucking cuts. The power head system mounts an AC motor which turns the chain drive sprocket via a torque transmitter. It also mounts the guide bar on a pair of linear bearings which are actuated by a small linear actuator via a load cell. This arrangement is shown in Figure 6. The load cell (mounted between the linear bearings) measures the reaction force between the drive sprocket and the guide bar, which are pulled together by two strands of the chainsaw chain. One half of this value is reported herein as the static chain tension. The load cell data is used by a PID controller which drives the linear actuator also labeled in Figure 6. This allows static chain tension to be a controlled variable in the presence of relative thermal expansion as well as physical wearing of the chain and bar assembly. The load cell data is low-pass filtered in order to separate mechanical vibration from thermal expansion and contraction. Also shown are pneumatically actuated position locks that remove the linear actuator from the chain tension load path during cutting operations, preventing backdrive. Because of the polygon effect of drive sprockets having few teeth (a six tooth sprocket was used), chain tension was adjusted while free running the chain at a low speed.

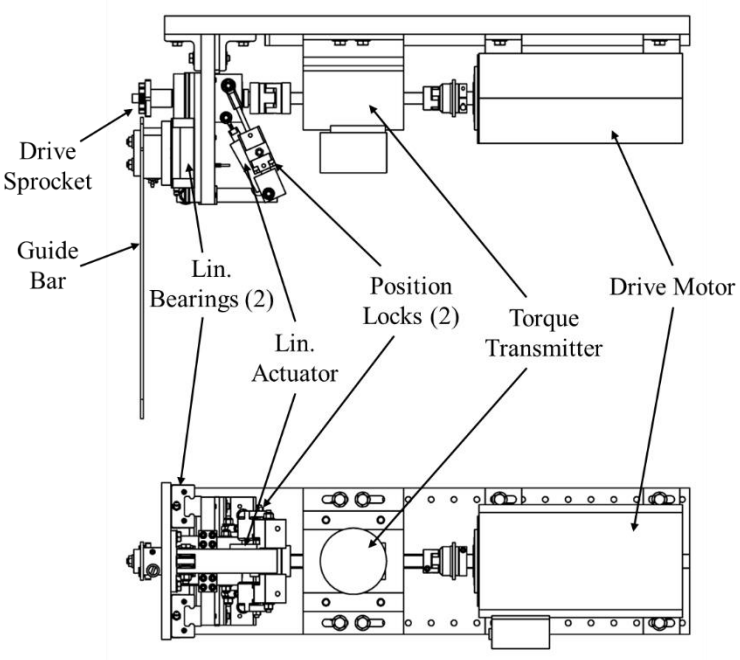

Figure 6: Power head system. Chain tension load cell resides between linear bearings.

The work holding assembly is depicted in Figure 7. It mounts a pneumatically actuated main clamp which holds the workpiece during cutting. The support for the main clamp incorporates two load cells. One is for measuring cutting force (force exerted horizontally by the chain on the workpiece, in the direction of the local chain velocity), and the other for measuring feed force (force exerted downward as the chain and bar are fed through the workpiece). Also included is a pneumatically actuated shuttle clamp, which together with the main clamp allows the workpiece to be indexed forward rapidly and automatically between successive cuts. Lastly an infrared (IR) spot sensor is mounted to measure temperature of the nose of the guide bar when the power head is in its retracted position between cuts. Both the shuttle

clamp and IR spot sensor are necessary for temperature-based cutting studies which require controlled timing between cuts, in addition to controlling cut parameters and the operating environment.

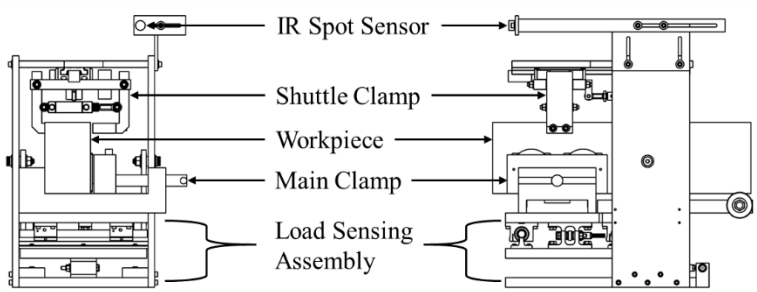

Figure 7: Work holding system.

The machine enclosure (not shown) incorporates a mount for an infrared camera oriented to view the guide bar. The camera is a FLIR A655sc, with 640 by 480 pixel detector and accuracy to ±3.6 °F when target emissivity is 0.95. Guide bars are prepared with aerosol paint having low reflectivity and emissivity equal to 0.95, taking care to mask surfaces the chain will slide on. Alignment markings are then machined onto the bar surface. The low emissivity of the bare steel surface allows the markings to be visible to the IR camera as an apparent temperature discontinuity throughout the operating temperature range of the guide bar. A prepared guide bar is shown in Figure 8. The thermal region of interest for this study is also shown in Figure 8, which was selected due to rapid wear rates and short thermal response times at that location.

Figure 8: Guide bar prepared for infrared photography. The superimposed arrow and circle show the thermal region of interest selected for comparison in this study.

The thermal response time can be thought of as how quickly the temperature reacts to a change in cutting conditions. This value varies with bar position, and can be visualized using non-dimensional temperature, T_{ND} (Eq. 7).

$$T_{ND} = \frac{T_t - T_i}{T_\infty - T_i} \tag{7}$$

Figure 9 is a plot showing non-dimensional temperature variation with bar position. For this result a chain and bar starting at room temperature were free run for 20 minutes with static chain tension controlled at 25 lb, shaft speed equal to 10,000 rev/min and a lubricant flow rate of 3 mL/min. T_i was taken as the initial measured temperature distribution and T_∞ was taken as the steady state temperature distribution at the end of the 20 minutes. The depicted T_{ND} distribution corresponds to 32 seconds of run time which is a typical value for the timing between cuts in the cutting tests.

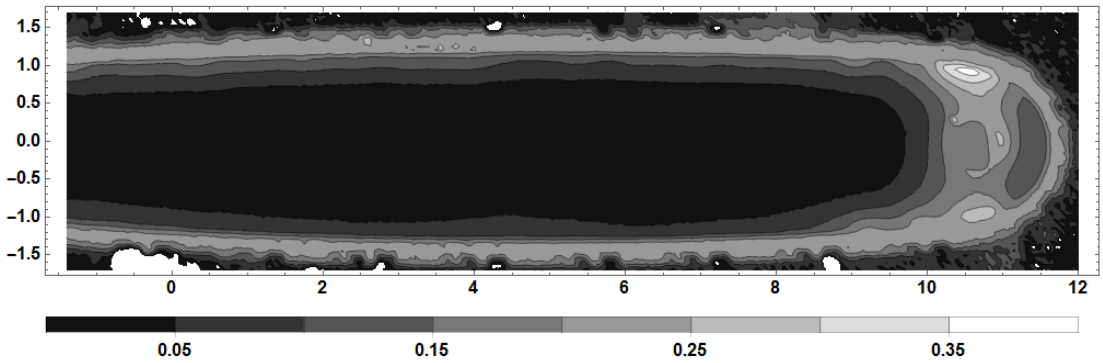

Figure 9: Distribution of T_{ND} on guide bar after 32 seconds of free running.

Another reason for choosing the nose tangency is the heavy wear that occurs there due to high angular acceleration of the passing chain links, as mentioned previously. Typical polishing and material loss in this region of the bar rails is shown in Figure 10.

Figure 10: Typical heavy wear at the nose tangency.

The cutting experiments were designed as follows. All cuts were nose-clear bucking. Manipulated factors were lubricant type, lubricant flowrate, and static chain tension. The eight lubricants under study are listed in Table 1, along with their cost per quart. Lubricant 1 is a petroleum based, purpose made guide bar lubricant.

Lubricants 2 through 5 are potential repurposed lubricants available to the opportunistic chainsaw operator. Lubricant 6 is lubricant 1 diluted 50% by volume with kerosene, which is reportedly used by some operators to improve pumping ability at extremely low temperatures. However ambient temperature was room temperature for all cutting tests. Lubricants 7 and 8 are two examples of vegetable based bar lubricants currently available in the U.S. domestic market. Table 2 lists a selection of physical properties measured for each lubricant. Viscosity numbers are kinematic viscosity in centistokes. Lubricant was supplied to the chain and bar assembly using a programmable peristaltic pump feeding the guide bar lubricant port.

Table 1: Lubricants under study and their costs.

Lubricant	Description	Cost per quart
1	CRC Bar and Chain Lubricant	$8.99
2	Formula Shell SAE 5W-30	$3.53
3	Used SAE 5W-30 Motor Oil	$0.00
4	Valvoline MaxLife ATF	$6.04
5	Mobil DTE 25 Hydraulic Oil	$9.10
6	Lubricant 1 with 50 vol% Kerosene	$5.67
7	G-Oil Bar and Chain Green Oil	$4.79
8	Motion Lotion Biodegradable Bar and Chain Oil	$6.00

Table 2: Lubricant physical properties and test methods.

Property	Method	Units	Lubricant							
			1	2	3	4	5	6	7	8
Specific Gravity	ASTM D1298	-	0.908	0.859	0.862	0.843	0.878	0.839	0.874	0.922
Flashpoint	ASTM D92	°F	381	457	370	442	450	-	388	619
	ASTM D93	°F	-	-	-	-	-	124	-	-
Pour Point	ASTM D97	°F	-22	-27	-38	<-38	-11	<-38	5	-22
Viscosity, 104 °F	ASTM D445	cSt	75.9	64.3	56.1	28.5	43.5	3.37	114	38.4
Viscosity, 212 °F	ASTM D445	cSt	8.5	11	9.34	5.96	6.56	1.44	26.2	8.74
Viscosity Index	ASTM D2270	-	77	164	134	148	101	102*	265	217

** Viscosity of lubricant 6 is below the recommended limit in ASTM D2270. Extrapolation was used.*

Table 3 lists the levels for lubricant flowrate and chain tension used for testing. Eight lubricants, four flowrates, and three chain tension levels along with three replicates at all factor combinations resulted in 288 total data cuts. While chain tension can be manipulated quickly between successive cuts, resident lubricant content in the chain and bar cannot. Due to this, lubricant type and lubricant flowrate were separated by experimental blocks. This resulted in 32 blocks, each of which was carried out with cuts on a single wood cant loaded into the test stand. Each block contains three replicates of all three chain tension levels, with run order randomized. Block order was also randomized. Shaft speed was 10,000 rev/min and depth of cut was 0.0058" (measured as the feed distance between passes of right-hand cutter links) for all cuts.

Table 3: Factor levels for lubricant flowrate and chain tension.

Level	Flowrate [mL/min]	Chain Tension (lb)
Warmup	Match block	25
1	1	10
2	3	20
3	5	30
4	10	--

Because a steady state bar temperature distribution is not reached during a single cut (as shown in Figure 9), a cut sequence was devised that controls the initial temperature distribution to an acceptable level. This cut sequence is depicted in Figure 11, which shows the cutting process for each cut and for each cant loaded in the test stand. Two minutes of free running followed by five warm-up cuts at the start of the cant bring the guide bar into its operating temperature range. Chain tension is

adjusted before every cut using the chain tension controller. Each data cut is the third in a triplet of cuts at identical parameters. By extending the amount of time spent at each combination of factor levels using these triplets of cuts, thermal responses were more pronounced and the dependency of temperature results on initial conditions was reduced. Data coming from the third triplet composes a single replicate in the study. Between each triplet of cuts, the IR spot sensor shown in Figure 7 was aligned with the nose region of the bar and used to indicate whether the bar was too hot or too cool to begin with the next triplet of cuts. The target temperature for this step was set to 165° F. If the nose temperature was below this value, the chain was free run at 12,000 rev/min and 30 lb of chain tension until the target temperature was reached. If the nose temperature was higher than the target, the test stand waited for the nose to cool down to the target temperature.

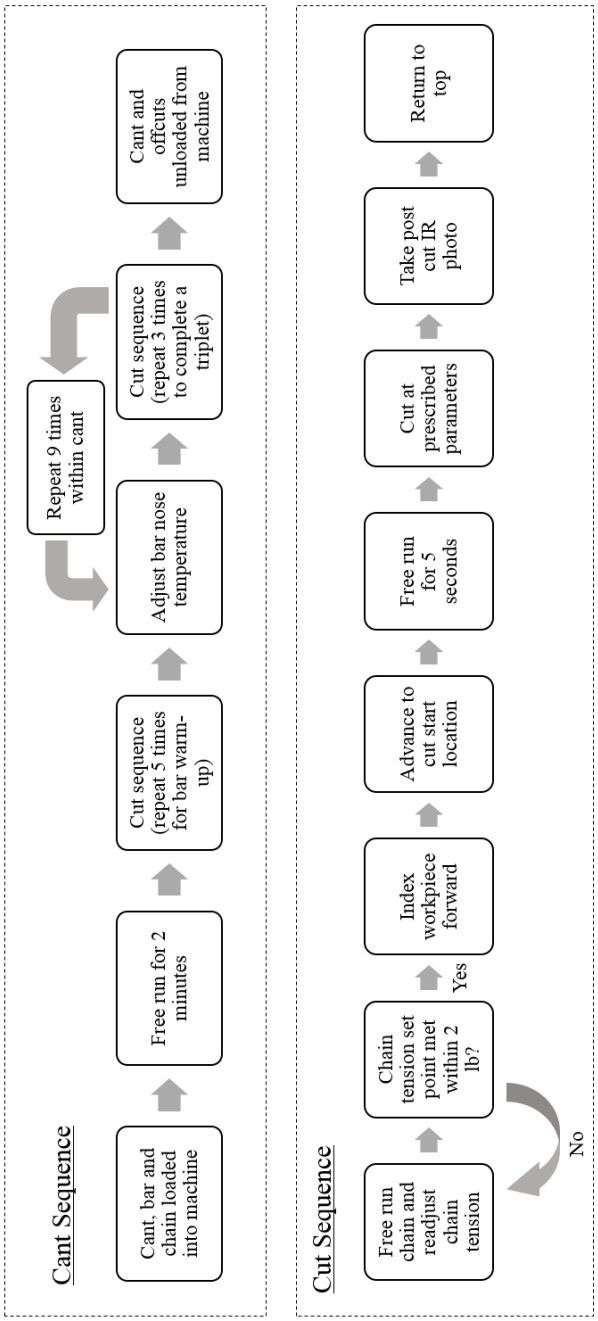

Figure 11: Ottomated sequences for entire cants and individual cuts used for cutting experiments.

A separate guide bar, chain, and lubricant supply tube for the peristaltic pump were dedicated to each lubricant type in order to prevent cross-contamination. The selected guide bar was the Oregon 140SXEA041 and the selected chain was Oregon 91PX set in loops with 52 drive links driven by a 6 tooth drive sprocket. Cants used in the study were rough sawn, green, clear Douglas Fir supplied by a local saw mill. Cross sections were 3.5” by 5.5” with 30” length. Lineal chainsaw cut spacing was set to 0.5”. Moisture content was measured with a Delmhorst J-2000 probe to have mean 33.5% and standard deviation 11.3%. All cants were above 27% moisture content with three outliers above 40% due to wet sapwood content. Wood density, measured for each cant with a tape measure and 40 lb capacity scale, was 46.8 lb/ft^3 with standard deviation 3.83 lb/ft^3. Exposed cross-sections after cutting of all 32 cants are shown in Figure 12.

Figure 12: Cross-sections of all 32 cants used in cutting testing.

Chapter 4: Free Running Test Apparatus, Methods and Consumables

This chapter describes the apparatus, methods and consumables used for the lubricant comparison tests that relied on free running. These tests focused on relating lubricant choice to physical wear of the chain. The same lubricants listed in Table 2 were compared. Free running was carried out on the same test stand as cutting tests. Wear of the chain was compared between trials by measuring increases in overall chain length. This is caused by material loss at the bearing surfaces shown in Figure 3, which increases the radial clearance at each rivet and therefore overall chain length. Length measurements were accomplished using a fixture with the test chain mounted on guides under a set amount of tension. Relative displacement of the guides measured with a dial indicator quantifies lengthening of the chain. Measurements are normalized for comparison in this document.

Three replicates (separate chains) were run for each lubricant. In order to produce results more representative of the bulk of the design life of these chains, all chains were first run-in using the following sequence:

1. Free run 5 minutes at 12,000 rev/min and 25 lb of chain tension with 2 mL/min flowrate of the lubricant designated for that chain and bar.
2. Free run 7 minutes at 12,000 rev/min and 30 lb of chain tension with 2 mL/min flowrate of the lubricant designated for that chain and bar.

Drive torque could be seen to spike during the 5 minute cycle, accompanied by peak temperatures. Drive torque and guide bar temperatures reduced to lower, steady state values during the 7 minute cycle, confirming that run-in was complete. After the run-in cycles, measurements of initial chain length for all 24 chains were taken. The wear cycle for each chain consisted of 30 minutes of free-running at 10,000 rev/min, 30 lb of chain tension and 0.22 mL/min flowrate of the lubricant under study. These are torturous conditions selected to cause boundary lubrication as described by region I of Figure 4. This recreates unintended circumstances encountered in the field such as pinching of the chain and bar, lubricant supply failures, or soil contamination of the chain and bar. All lubricants produced smoke in these conditions. After the wear cycles, a final length measurement was taken for all chains.

The guide bars were the same eight previously used in cutting testing, still paired with their designated lubricant. Chains were again Oregon 91PX set in 52 drive link loops, originally new before their run-in cycles and driven by a 6 tooth drive sprocket.

Chapter 5: Cutting Test Results and Discussion

Effect of Cutting

Variation in test results pertaining to lubrication performance due to the stochasticity of wood cutting must be evaluated. Typical results for the variation in drive torque, feed force, cutting force and chain tension during an individual cut are shown in Figure 13. These traces have been filtered using a second order Butterworth low-pass filter with 5.0 Hz cutoff frequency to remove mechanical vibration noise and facilitate discussion. Data acquisition begins during free running operation in order to measure free running torque and actual chain tension. Free running values for torque and chain tension are taken as means from time equal to zero seconds until the ‘o’ on the abscissa. Cutting values of torque, cutting force, feed force and chain tension are taken as the mean between the two ‘x’ marks.

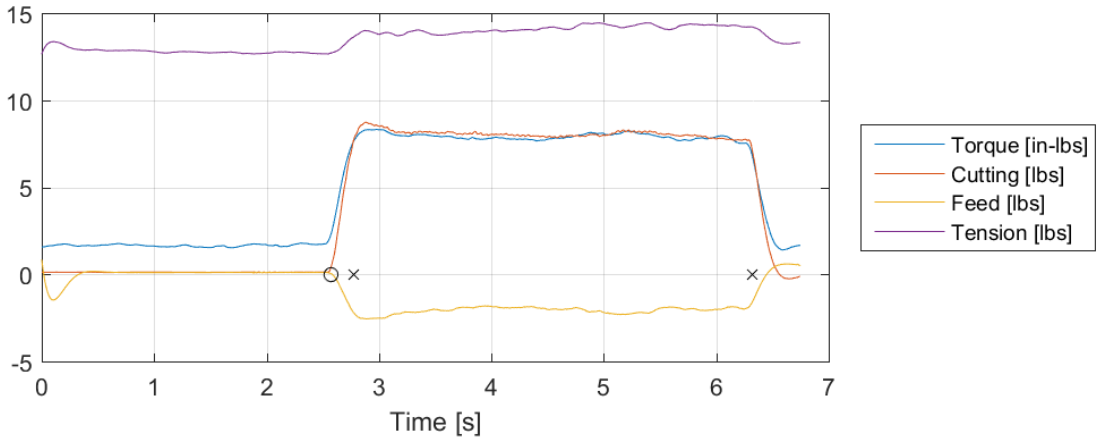

Figure 13: Low-pass filtered load and torque data measured during a typical cut. The ‘x’ marks on the abscissa mark cut start and finish times.

The proportion of shaft power consumed due to cutting (R_{cut} in Eq. 5) had mean 70.7% with standard deviation 2.7% for all 288 cuts. This shows power consumption was dominated by cutting, not friction internal to the chain and bar assembly. Mean cutting force of each cut did not correlate with moisture content or density of the wood cants. However it is expected that the variation in cutting force could be predicted if mechanical properties of the cants were known, as demonstrated by Naylor [21].

Furthermore, post cut bar temperature at the nose tangency did not correlate with cutting force, but did correlate strongly with free running torque. This contrast is shown graphically in Figure 14, with R^2 values listed for linear least-squares regressions. The low correlation in the top plot indicates variation in machinability of the wood cants (caused by natural variation in wood properties) produced little effect on power dissipation due to friction within the chain and guide bar assembly. The better correlation between post cut temperature and free running torque is as expected; more shaft power dissipated by friction resulted in higher bar temperatures.

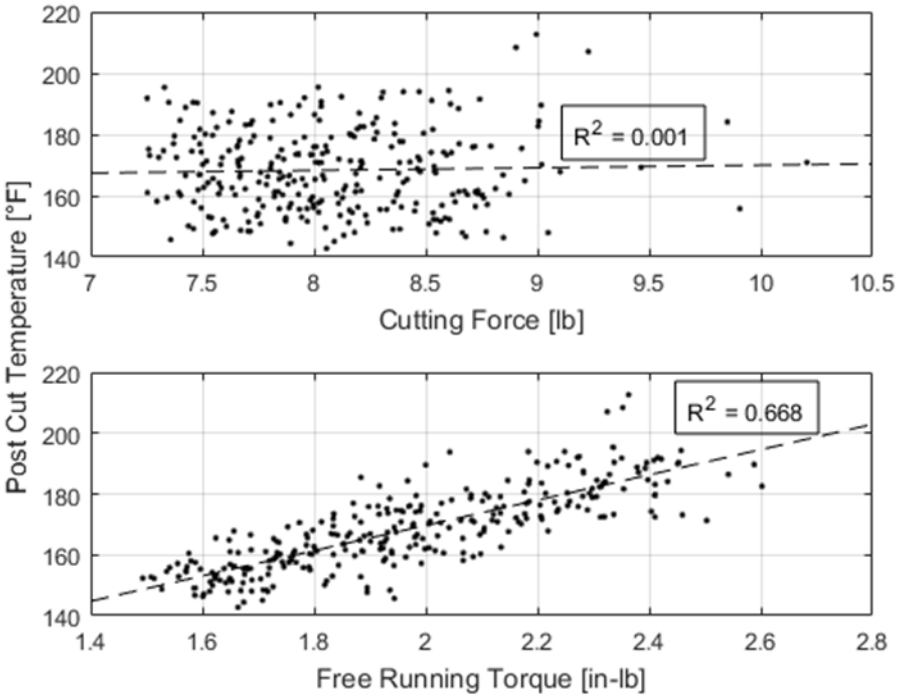

Figure 14: Correlations of bar temperature with cutting force (top) and bar temperature with free running torque (bottom) for all data cuts. R^2 values are listed for a linear least-squares regression. No correlation in the top plot indicates variation in wood properties did not affect power dissipation due to internal friction in the chain and bar. Good correlation was found between free running torque and frictional heating of the bar.

Effect of Chain Tension

The ability of the chain tensioner to control chain tension is shown in Figure 15. Measured chain tension is taken as the mean value of chain tension during free running prior to a cut. The reason for these errors include steady state error of the control system, incremental offset due to the chain tension pneumatic locks engaging, relative thermal strain of the chain and bar between locking the chain tensioner and making the cut, and variation in chain tension due to changes in shaft speed.

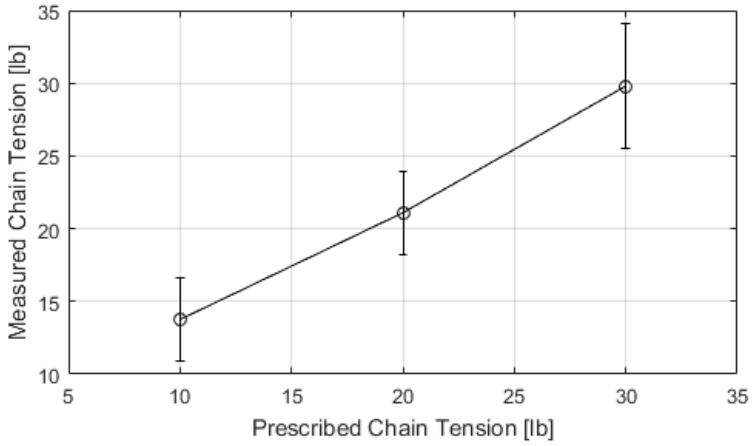

Figure 15: Variation between prescribed and measured chain tension for all data cuts. Error bars are ± 1.96 standard deviations for n = 96 cuts at each prescribed chain tension level.

The dependence of free running torque on chain tension is shown for all data cuts in Figure 16. $R^2 = 0.847$ for a linear least squares regression shows how strongly chain tension dictates power dissipation due to friction in the chain and bar assembly, even without accounting for prescribed variation in lubricant type and flowrate between cuts. This result aligns with the expectation that chain tension effects the contact pressure between all bearing surfaces in the chain and bar assembly, which will increase power dissipation if bearing friction coefficients and sliding velocities are held constant, as predicted by Eq. 6.

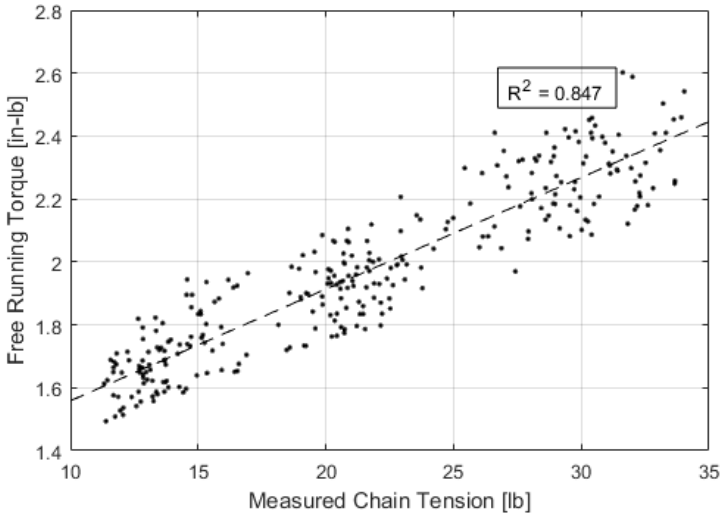

Figure 16: Correlation of free running torque with measured chain tension for all data cuts. R^2 = 0.847 for a linear least-squares regression without accounting for variation in lubricant or lubricant flowrate between cuts.

Effects of Lubricant Type and Flowrate

Separating the effects of chain tension, lubricant type and lubricant flowrate indicates that a mixture of all three lubrication regimes described in the adapted Stribeck curve of Figure 4 occurred within the parameters of the cutting tests. The graphs of Figures 17-20 depict the correlation between lubricant viscosity and post cut temperature. Viscosity index values are taken from Table 2 and all error bars are ±1.96 standard deviations from the mean for three replicates per data point. Temperature is dependent on viscosity index only for flowrates of 3 and 5 mL/min. This appears to indicate that at the chosen set of cutting parameters, 1 mL/min causes primarily boundary lubrication on bearing surfaces (indicated by a lack of dependence on viscous properties of the lubricant, since no film exists). For lubricant flowrates of 3 and 5 mL/min, the post cut temperature dependence on viscosity index

shows that this property helps determine how often a lubricant film exists, indicating that these cutting parameters produce the mixed lubrication regime shown in Figure 4. Finally at a flowrate of 10 mL/min, viscosity index ceases impacting post cut temperature. This indicates that 10 mL/min of lubricant flow created a well-developed film lubrication regime to the right of the plot in Figure 4, since a robust film exists regardless of the viscous properties of the lubricant.

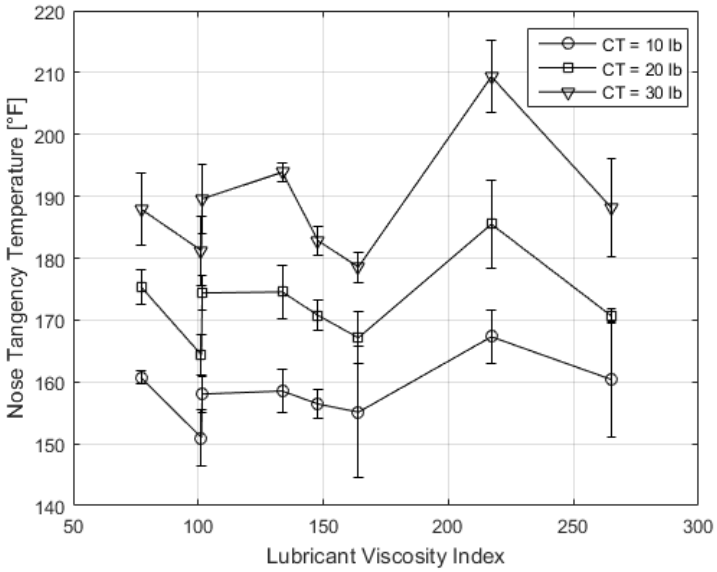

Figure 17: The lack of effect of viscosity index on post cut temperature at flowrate 1 mL/min, grouped by prescribed chain tension. Error bars are ±1.96 standard deviations for 3 replicates.

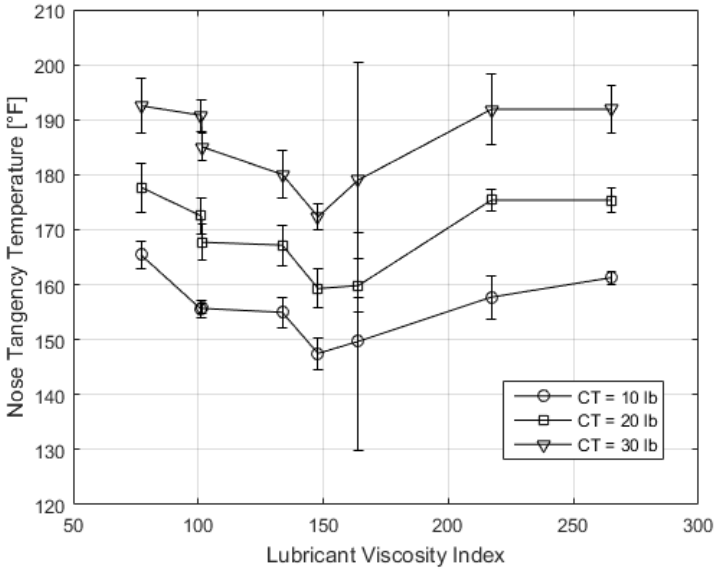

Figure 18: The effect of viscosity index on post cut temperature at flowrate 3 mL/min, grouped by prescribed chain tension. Error bars are ±1.96 standard deviations for 3 replicates.

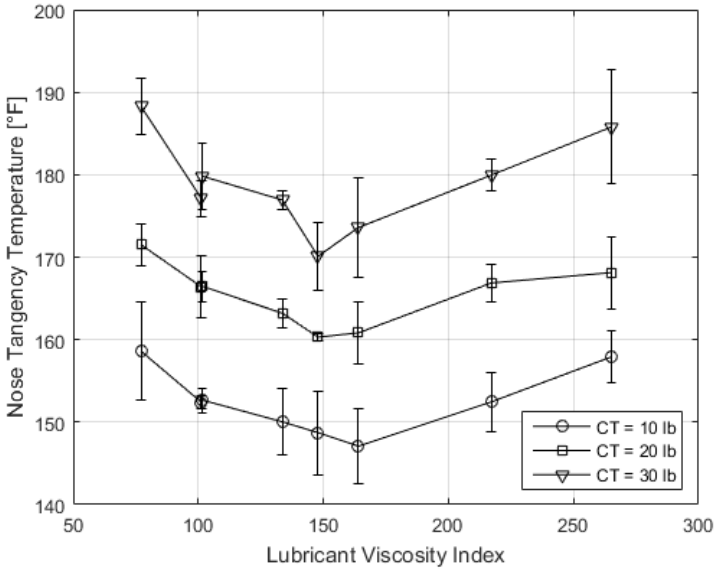

Figure 19: The effect of viscosity index on post cut temperature at flowrate 5 mL/min, grouped by prescribed chain tension. Error bars are ±1.96 standard deviations for 3 replicates.

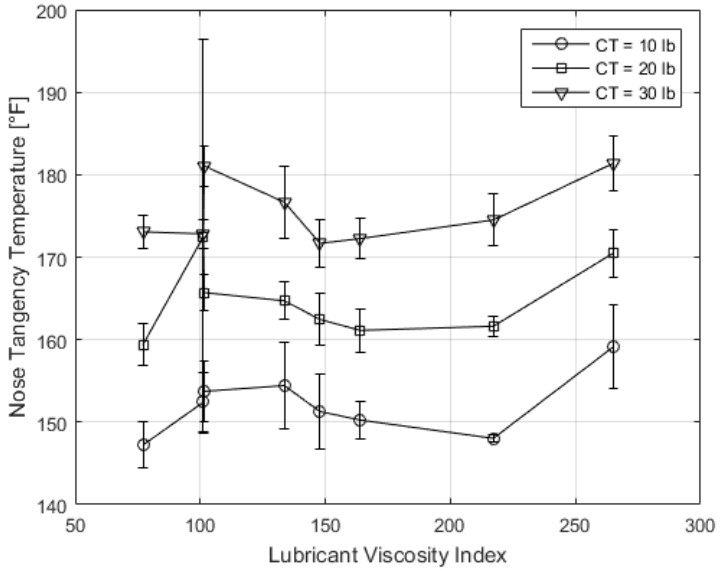

Figure 20: The lack of effect of viscosity index on post cut temperature at flowrate 10 mL/min, grouped by prescribed chain tension. Error bars are ±1.96 standard deviations for 3 replicates.

For flowrates of 3 and 5 mL/min, viscosity index correlates with post cut temperatures better than the kinematic viscosity values given in Table 2. This may be because the film temperatures in the chain and guide bar are much higher than the temperatures selected for viscosity testing. It is also important to note that optimizing viscosity index for a lubricant based solely on post cut temperature may not yield the superior lubricant with respect to wear prevention. As shown in Figure 4, a robust lubricant film on the right side of the diagram can viscously dissipate more power than a mixed lubrication regime while being more protective of bearing surfaces.

Chapter 6: Free Running Test Results and Discussion

Results from free running wear testing are shown in Figure 21. Extension of chains due to the wear cycle are given with error bars showing ±1.96 standard deviations from the mean for each lubricant. Under the boundary lubrication conditions created by the wear test cycles, a discernable performance difference arises between some of the lubricants. Increase in chain length did not correlate with any of the lubricant properties listed in Table 2. This is most likely due to the fact that very limited information was available about additives in each of the lubricants, which dictate friction coefficients and wear rates in the boundary lubrication regime.

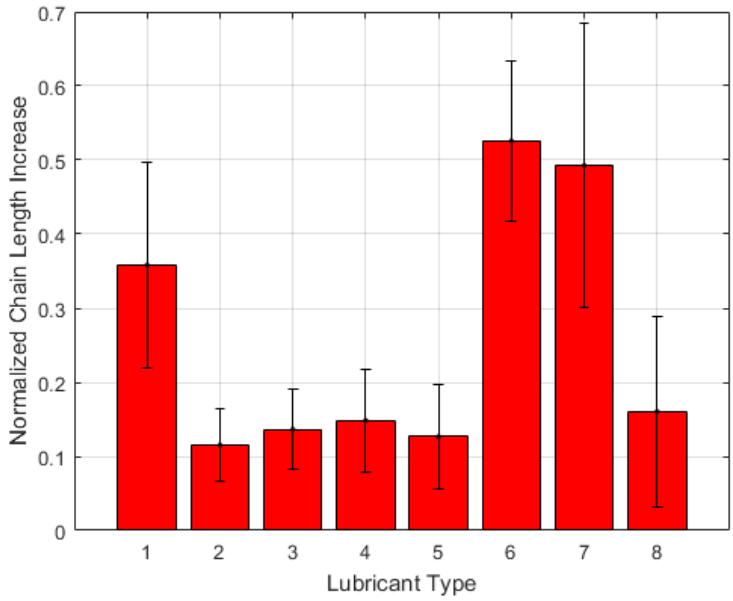

Figure 21: Increase in chain length caused by 30 minute wear cycle, grouped by lubricant. Error bars are ±1.96 standard deviations from the mean for 3 replicates.

Lubricants 1, 6 and 7 showed high wear rates and high variability between replicates. Since Lubricant 6 is a diluted version of lubricant 1 with 50 vol. %

kerosene added, its ability to deliver boundary additives to the bearings surfaces seems to have been correspondingly decreased, thereby raising the wear rate. Lubricant 7 is a vegetable based lubricant with high values for viscosity and viscosity index. Without a fluid film available, the boundary additives in this lubricant appear to be low performance for the bearing materials of the chain and bar. Lubricants 2-5 are all name brand petroleum based lubricants that most likely all have highly developed additive packages. Interestingly, little to no discernable difference between lubricants 2 and 3 (new and used SAE 5W-30 engine lubricant, respectively) appeared under these test conditions. However lubricant 3 was quite messy and odorous. Lubricant 8 uses a vegetable based and produced high performance similar to lubricants 2-5, indicating an effective additive combination.

Figure 22 shows the correlation between chain extension and average drive torque during the wear cycle. The positive correlation shows that in the boundary lubrication regime, plasticity and surface modification produced a measurable effect on power consumption.

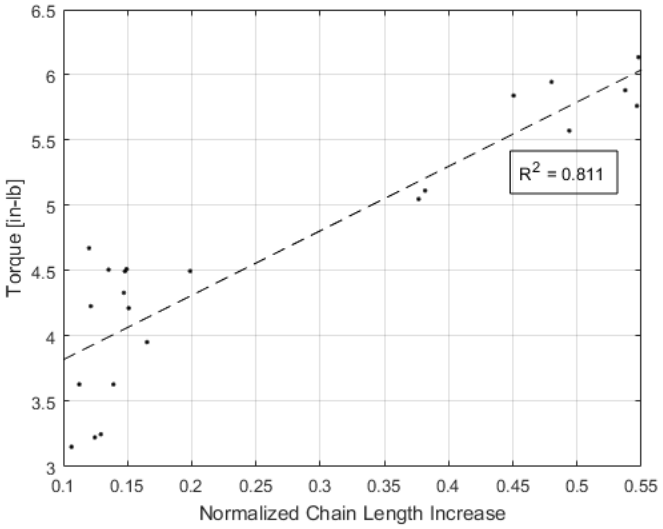

Figure 22: Correlation between increase in chain length and drive torque during the free running wear cycles. R^2 = 0.811 for a linear least-squares regression.

Chapter 7: Conclusions

This study identified performance differences in a variety of available chainsaw guide bar lubricants using two types of tests. The first was a cutting test designed to model normal usage of a handheld chainsaw during bucking cuts while exploiting the high variable control available in a laboratory setting. The second was a free running test designed to model rapid wear conditions caused by rough field usage. Previous literature has been able to list the physical property differences between available lubricants as well as differences in guide bar temperature during free running of a chainsaw in a laboratory setting. In contrast, data from previously published field studies that involved wood cutting struggled to discern differences in lubricant performance due to lack of variable control.

During cutting tests, it was found that while overall power consumption was dominated by the cutting operation, results for bar temperature showed that variation in cutting performance had little effect on power dissipation due to friction internal to the chain and bar assembly. Of the manipulated variables of the cutting study, chain tension was found to have the strongest effect on this internal frictional power dissipation, as indicated by measurements of free running driveshaft torque and bar temperatures after each cut was completed. It was also found that viscosity index of each lubricant correlated with post cut bar temperature only for lubricant flow rates of 3 mL/min and 5 mL/min, which indicates a mixed lubrication regime. The lack of correlation at 1 mL/min indicates the existence of chiefly boundary lubrication

conditions in the chain and bar assembly, and the lack of correlation at 10 mL/min indicates fully developed film lubrication conditions regardless of which lubricant is chosen.

Free running tests isolated each lubricant's ability to protect the bearing surfaces of the saw chain under boundary lubrication conditions. These conditions isolate the performance of antiwear additives in each lubricant, rather than their viscosity characteristics. It was found that the additive combination in name-brand, petroleum based lubricants designed for a variety of applications effectively slowed the rate of chain wear. It was also found that vegetable based lubricants are capable of a similar level of performance only given a proper additive blend. Lastly, the petroleum based lubricant advertised specifically as a bar and chain lubricant was found to have poor boundary lubrication performance. It should be noted that this product survey does not necessarily represent all available lubricants marketed for the application.

Now that the relative effects of lubricant choice, chain tension, and lubricant flowrate have been established, future work could concentrate on a longer term cutting study focused only on lubricant selection. The longer duration would allow measurable levels of chain extension to occur under mixed and film lubrication conditions, thereby allowing the direct comparison of guide bar temperature distributions with component wear rates. Another recommended avenue of continued work is to select test conditions that once again cause boundary lubrication while

comparing lubricants with completely known additive blends. Bearing surface inspection could also be a useful tool.

Bibliography

[1] M. Schullian, “The Chain Osteotome by Heine,” *J. Hist. Med. Allied Sci.*, vol. 35, no. 4, pp. 454–459, 980.

[2] J. Wardrop, “British Columbia ’ s Experience with Early Chain Saws,” *Mater. Cult. Rev.*, vol. 2, pp. 5–10, 1976.

[3] J. W. Challenger, “Power Saw Performance Analyzed,” *Br. Columbia Lumberm.*, vol. 25, no. 2, pp. 29–30, 1941.

[4] W. C. Randel, “Cutting characteristics of different power saw chain designs,” *Michigan Quaterly Bull.*, vol. 35, no. 2, pp. 219–229, 1952.

[5] A. Rac and A. Vencl, “Performance investigation of chain saw lubricants based on new sunflower oil (NSO),” in *ÖTG-Symposium 2008*, 2008, pp. 249–257.

[6] A. Skoupy, B. Pechlak, and P. Sejkora, “A Contribution to the understanding of oil dispersion at the work with a chain saw by means of the radiotracer method,” *Lesnictví*, vol. 36, no. 11, pp. 937–946, 1990.

[7] J. C. J. Bart, S. Cavallaro, and E. Gucciardi, *Biolubricants: Science and technology*, 1st ed. Philadelphia: Woodhead, 2013.

[8] R. Popovici, “Estimating chainsaw operating costs based on fuel , lubricants and spare parts,” vol. 6, no. 1, 2013.

[9] S. Boyde, “Green Lubricants. Environmental Benefits and Impacts of Lubrication,” *Green Chem.*, vol. 4, no. 4, pp. 293–307, 2002.

[10] A. Hartweg and P. K. Keilen, “The environmental benevolence of biological oils,” *Scottish For.*, vol. 43, no. 4, pp. 311–317, 1989.

[11] D. Ruppert, “Umweltfreundliche Motorsägen-Kettenschmiermittel (Environmentally friendly chain saws - chain lubricant obtained the Ecolabel).”

[12] G. Stachowiak and A. W. Batchelor, “Hydrodynamic Lubrication,” in *Engineering Tribology, 3rd Ed.*, 2011, pp. 103–113.

[13] O. N. Anand and V. K. Chhibber, “Vegetable oil derivatives: Environment-friendly lubricants and fuels,” *J. Synth. Lubr.*, vol. 23, no. 2, pp. 91–107, 2006.

[14] J. Li, Z. Li, T. Ren, X. Zeng, and E. Van Der Heide, “Hydrolytic stability and tribological properties of N-containing heterocyclic borate esters as lubricant additives in rapeseed oil,” *Tribol. Int.*, vol. 73, pp. 101–107, 2014.

[15] J. Salimon, N. Salih, and E. Yousif, “Chemically modified biolubricant basestocks from epoxidized oleic acid: Improved low temperature properties and oxidative stability,” *J. Saudi Chem. Soc.*, vol. 15, no. 3, pp. 195–201, 2011.

[16] J. W. Oehrli, “Cutting Action of Chain-Saw Teeth,” *For. Prod. J.*, vol. 10, no. 1, pp. 4–7, 1960.

[17] G. Pahlitzsch and H. Peters, “Aspects of Chain Saw Cutting,” in *Proceedings of a conference held at the University of California Forest Products Laboratory*, 1966, pp. 38–45.

[18] D. T. Priest, “The testing of chain saws,” *Commonw. For. Rev.*, vol. 43, no. 3, pp. 246–250, 1964.

[19] S. C. Gambrell and E. F. Byars, “Cutting Characteristics of Chain Saw Teeth,” *For. Prod. J.*, vol. 16, no. 1, pp. 62–71, 1966.

[20] D. D. Reynolds, W. Soedel, and C. Eckelman, “Cuting Characteristics and Power Requirements of Chain Saws,” *For. Prod. Journal1*, vol. 20, no. 10, pp. 28–35, 1970.

[21] A. Naylor, P. Hackney, N. Perera, and E. Clahr, “A PREDICTIVE MODEL FOR THE CUTTING FORCE IN WOOD MACHINING DEVELOPED USING MECHANICAL PROPERTIES,” *Bioresources*, vol. 7, no. 3, pp. 2883–2894, 2012.

[22] A. Otto and J. Parmigiani, “Velocity, Depth-of-Cut, and Physical Property Effects on Saw Chain Cutting,” *Bioresources*, vol. 10, no. 4, pp. 7273–7291, 2015.

[23] L.-E. Stacke, “Cutting Action of Saw Chains,” Chalmers University of Technology, 1989.

[24] M. Stanovský, J. Schürger, M. Jankovský, V. Messingerová, R. Hnilica, and M. Kučera, “The Effect of Lubricating Oil on Temperature of Chainsaw Cutting System,” pp. 83–90.

[25] T. Nordfjell, L. Johansson, and R. Gref, “A Method to Measure Saw-Chain Lubrication,” vol. 18, no. March 2006, pp. 41–45, 2007.

[26] P. De Caro, A. Gaset, and N. N. The, “Vegetable base lubricants in forestry: Results from a test campaign,” *Teknoscienze*, vol. 12, no. 4, pp. 26–30, 2001.